European Journal of Cancer (2012) **48**, 1244–1254

Available at www.sciencedirect.com

SciVerse ScienceDirect

journal homepage: www.ejconline.com

Relationship between ^{18}F-FDG uptake on positron emission tomography and molecular biology in malignant pleural mesothelioma

Kyoichi Kaira [a,*], Masakuni Serizawa [b], Yasuhiro Koh [b], Toshiaki Takahashi [a], Hirofumi Hanaoka [e], Noboru Oriuchi [f], Masahiro Endo [g], Haruhiko Kondo [c], Takashi Nakajima [d], Nobuyuki Yamamoto [a]

[a] *Division of Thoracic Oncology, Shizuoka Cancer Center, 1007 Shimonagakubo Nagaizumi-cho, Sunto-gun, Shizuoka 411-8777, Japan*
[b] *Division of Drug Discovery and Development, Shizuoka Cancer Center Research Institute, 1007 Shimonagakubo Nagaizumi-cho, Sunto-gun, Shizuoka 411-8777, Japan*
[c] *Division of Thoracic Surgery, Shizuoka Cancer Center, 1007 Shimonagakubo Nagaizumi-cho, Sunto-gun, Shizuoka 411-8777, Japan*
[d] *Division of Pathology, Shizuoka Cancer Center, 1007 Shimonagakubo Nagaizumi-cho, Sunto-gun, Shizuoka 411-8777, Japan*
[e] *Department of Bioimaging Information Analysis, Gunma University Graduate School of Medicine, Showa-machi, Maebashi, Gunma 371-8511, Japan*
[f] *Department of Diagnostic Radiology and Nuclear medicine, Gunma University Graduate School of Medicine, Showa-machi, Maebashi, Gunma 371-8511, Japan*
[g] *Division of Diagnostic Radiology, Shizuoka Cancer Center, 1007 Shimonagakubo Nagaizumi-cho, Sunto-gun, Shizuoka 411-8777, Japan*

Available online 11 February 2012

KEYWORDS
^{18}F-FDG PET
Mesothelioma
Glut1
Hypoxia
mTOR

Abstract *Background:* The usefulness of 2-[^{18}F]-fluoro-2-deoxy-D-glucose (^{18}F-FDG) positron emission tomography (PET) can help for predicting the therapeutic response and outcome in malignant pleural mesothelioma (MPM). However, no satisfactory biologic explanation exists for this phenomenon. The aim of this study is to investigate the underlying biologic mechanisms of ^{18}F-FDG uptake.

Methods: Twenty-one patients with MPM who underwent ^{18}F-FDG PET before treatment were included in this study. Tumour sections were stained by immunohistochemistry for glucose transporter 1 (Glut1); glucose transporter 3 (Glut3); hypoxia-inducible factor-1 alpha (HIF-1α); hexokinase I; vascular endothelial growth factor (VEGF); microvessels (CD34); epidermal growth factor receptor (EGFR); cell proliferation (Ki-67 labelling index); Akt/mTOR signalling pathway (PTEN, p-Akt, p-mTOR and p-S6K); cell cycle control (p53 and pRb); apoptosis marker (bcl-2). We also conducted an *in vitro* study of ^{18}F-FDG uptake in mesothelioma cell lines.

Results: ^{18}F-FDG uptake was significantly correlated with Glut1 ($p < 0.0001$), HIF-1α ($p = 0.006$), hexokinase I ($p = 0.0002$), VEGF ($p = 0.0013$), CD34 ($p = 0.0001$),

* *Corresponding author:* Tel.: +81 55 989 5222; fax: +81 55 989 5634.
E-mail address: kkaira1970@yahoo.co.jp (K. Kaira).

0959-8049/$ - see front matter
doi:10.1016/j.ejca.2012.01.016

Ki-67($p = 0.0047$), mTOR ($p = 0.00478$) and p53 ($p = 0.0004$). High uptake of ^{18}F-FDG was significantly associated with poor outcome in MPM. Our *in vitro* study showed that upregulation of Glut1 and HIF-1α was closely related with ^{18}F-FDG uptake into mesothelioma cell, and mTOR inhibitor induced a decrease in Glut1 expression and ^{18}F-FDG uptake.
Conclusion: The amount of ^{18}F-FDG uptake in MPM is determined by the presence of glucose metabolism, phosphorylation of glucose, hypoxia, angiogenesis, cell proliferation (Ki-67), cell cycle regulator, and mTOR signalling pathway.

1. Introduction

Malignant pleural mesothelioma (MPM) is an aggressive tumour with a poor prognosis and an increasing incidence in many countries. Recently, the usefulness of 2-[^{18}F]-fluoro-2-deoxy-D-glucose (^{18}F-FDG) positron emission tomography (PET) for the diagnosis of MPM has been investigated in some studies.[1–4] ^{18}F-FDG PET has proved useful in detecting malignant pleural lesions[5] and assessing treatment efficacy in MPM.[4] Moreover, ^{18}F-FDG PET is also described to help predicting the prognosis of MPM.[6] However, there is still no data about the possible mechanisms for ^{18}F-FDG uptake in MPM.

Determination of malignant lesions with ^{18}F-FDG PET is based on the glucose metabolism.[7,8] The overexpression of glucose transporter 1 (Glut1) has been shown to be closely related to ^{18}F-FDG uptake in human cancer.[7,8] Glut 1 is thought to be a possible intrinsic marker of hypoxia, and the expression of Glut 1 has been found to be regulated by hypoxia in a hypoxia inducible factor (HIF)-1-dependent way.[9,10] Previous studies suggest that hypoxic conditions correspond to a higher ^{18}F-FDG uptake.[11,12] In addition, several researchers described the relationship between ^{18}F-FDG uptake and the expression of vascular endothelial growth factor (VEGF) or micro-vessel density (MVD).[13,14] HIF-1α is considered to support tumour growth by the induction of angiogenesis via the expression of the VEGF and also by high and anaerobic metabolic mechanisms.[15] Recent preliminary report demonstrated that ^{18}F-FDG PET could be a valuable tool for assessing the effects of the mammalian target of rapamycin (mTOR) inhibition in lung cancer patients.[16] mTOR is a downstream component of the PI3K/AKT pathway involved in the regulation of cell proliferation, angiogenesis, and metabolism. However, there is no report about the relationship between ^{18}F-FDG uptake within tumour cells and PI3K/AKT/mTOR signalling pathway in human neoplasms. As many factors can influence the extent of ^{18}F-FDG uptake, the underlying mechanisms for ^{18}F-FDG accumulation are still a matter of debate in various human neoplasms. Defining a correlation between these biomarkers and ^{18}F-FDG uptake may lead to a better understanding and interpretation of ^{18}F-FDG PET scanning in MPM. Moreover, the molecular biology including epidermal growth factor receptor (EGFR), cell cycle control (p53 and Rb) and apoptosis (bcl-2), has been described to play an important role in the pathogenesis of MPM.[17] We conducted ^{18}F-FDG PET studies and immunohistochemical analyses in patients with MPM. *In vitro* studies were also performed to investigate the possible mechanisms of ^{18}F-FDG uptake.

2. Material and methods

2.1. Patients

Between August 2003 and May 2009, 25 consecutive patients with MPM who underwent ^{18}F-FDG PET were analysed in this study. Of these patients, four patients were excluded for further studies because the tissue specimen was not available. Thus, a total of 21 patients were analysed in the study. The study protocol was approved by the institutional review board.

The median age of the patients was 66 years (range, 19–79 years). Eighteen patients were men and three were women. Eleven of the 21 patients underwent surgical resection, six patients surgical biopsy and the remaining four patients only percutaneous needle-core biopsy. Disease stage was classified according to the TNM staging system proposed by the International Mesothelioma Interest Group (IMIG).[18] Sixteen patients had the histology of epithelial type, two of biphasic type, one of sarcomatous type, and two of desmoplastic type. Of the total patients, 8, 1, 5 and 7 had stage I, II, III and IV tumours, respectively. As the initial treatment, 11 patients underwent surgery, five patients underwent systemic chemotherapy, two underwent thoracic radiotherapy and three patients had best supportive care alone. If including neoadjuvant therapy or relapse after surgery, 17 of 21 patients had systemic chemotherapy.

2.2. ^{18}F-FDG PET imaging

Patients fasted for at least 4 h before ^{18}F-FDG PET examination. Patients received an intravenous injection of 200–250 MBq of fluoro-2-deoxy-D-glucose and then rested for approximately 1 h before undergoing imaging.[19] Image acquisition was performed using an Advance NXi PET scanner and Discovery PET-CT scanner (GE Medical Systems, Milwaukee, WI, United

States). Two-dimensional emission scanning was performed from the groin to the top of the skull. PET/computed tomography image was independently reviewed by two experienced physicians. Acquired data were reconstructed by iterative ordered subset expectation maximisation. To evaluate ^{18}F-FDG accumulation, the tumour was first examined visually, and then the peak standardised uptake value (SUV) of the entire tumour was determined. The region of interest (ROI), measuring 3 cm in diameter, was set at the mediastinum at the level of the aortic arch and the mean SUV of the mediastinum was calculated. Finally, the T/M ratio, which is the ratio of the peak SUV of the tumour to the mean SUV of the mediastinum, was determined for each patient (Fig. S1).

2.3. Immunohistochemical staining

Immunohistochemical staining was performed according to the procedure described in the previous reports.[14,19–22] The following antibodies were used: a rabbit polyclonal antibody against GLUT1 (AB15309, Abcam, Tokyo, Japan, 1:200 dilution); a rabbit polyclonal antibody against GLUT3 (AB15311, Abcam, Tokyo, Japan, 1:100 dilution); a rabbit monoclonal antibody against hexokinase I (AB55144, Abcam, Tokyo, Japan, 1:200 dilution); a mouse monoclonal antibody against HIF-1α (NB100-123, Novus Biologicals, Inc., Littleton, 1:50 dilution); a murine monoclonal antibody against MIB-1 (Dako, Denmark, 1:40 dilution); a monoclonal antibody against VEGF (Immuno-Biological Laboratories Co., Ltd., Japan, 1:300 dilution) a mouse monoclonal antibody against CD34 (Nichirei, Tokyo, Japan, 1:800 dilution); a mouse monoclonal antibody against p53 (D07; DAKO, 1:50 dilution); a mouse monoclonal antibody against bcl-2 (Dako,1:100 dilution); a mouse monoclonal antibody against EGFR (Novovastra laboratories Ltd., Newcastle, United Kingdom, 1:100 dilution); a rabbit monoclonal antibody against PTEN (Cell signaling, 50 dilution); a rabbit polyclonal antibody against phosph-AKT (Abcam, Tokyo, Japan, 1:200 dilution); a rabbit monoclonal antibody against phosph-mTOR (Cell signaling, 80 dilution); a rabbit monoclonal antibody against phosph-S6K (Cell signaling, 100 dilution) and a mouse monoclonal antibody against Rb (Rb1, Dako, USA; 80 dilution).

The expression of Glut1, Glut3 and EGFR was considered positive if distinct membrane staining was present. Five fields (×400) were analysed to determine the frequency of the HIF-1α stained nuclei and hexokinase I stained cytoplasm. For Glut1, Glut3, EGFR, HIF-1α and hexokinase I, a semi-quantitative scoring method was used: 1 = <10%, 2 = 10–25%, 3 = 25–50%, 4 = 51–75% and 5 = >75% of cells positive. The tumours in which stained tumour cells made up more than 25% of the tumour were graded as positive.

The expression of VEGF was quantitatively assessed according to the percentage of immunoreactive cells in a total of 1000 neoplastic cells. The number of CD34-positive vessels was counted in four selected hot spots in a ×400 field (0.26 mm^2 field area). Microvessel density (MVD) was defined as the mean count of microvessels per 0.26 mm^2 field area.

For p53, microscopic examination for the nuclear reaction product was performed and scored. According to previous report,[21] p53 expression in more than 10% of tumour cells was defined as high expression. Expression of bcl-2 was considered to be positive if there was staining of area of the epithelial component of the tumour.

For, Ki-67, a highly cellular area of the immunostained sections was evaluated. All epithelial cells with nuclear staining of any intensity were defined as positive. Approximately 1000 nuclei were counted on each slide. Proliferative activity was assessed as the percentage of MIB-1-stained nuclei (Ki-67 labelling index) in the sample.

p-AKT, p-mTOR, p-S6K and Rb were considered positive if membranous and/or cytoplasmic staining was present, and PTEN was positive if nuclear staining. For p-AKT, p-mTOR, p-S6K, Rb and PTEN, a semi-quantitative scoring method was used: 1 = <10%, 2 = 10–25%, 3 = 25–50%, 4 = 51–75% and 5 = >75% of cells positive. The tumours in which stained tumour cells made up more than 25% of the tumour were graded as positive.

Sections were assessed using a light microscopic in a blinded fashion by at least two of the authors.

2.4. In vitro study

In vitro ^{18}F-FDG uptake study, growth-inhibition assay and immunoblot analysis were performed on MSTO-211H, NCI-H28 and NCI-H2052 (malignant mesothelioma cells) according to the established procedures.[23–28]

2.5. Cell culture

Human malignant mesothelioma cell lines MSTO-211H, NCI-H28 and NCI-H2052 were purchased from Japanese Cancer Research Resources (Tokyo, Japan) and were maintained in RPMI-1640 medium supplemented with 10% FBS. The cell lines were grown in a humidified atmosphere containing 5% CO_2 at 37 °C.

2.6. Reagents

Cobaltous chloride ($CoCl_2$) was purchased from *Wako* Pure Chemical Industries (Osaka, Japan). Cytochalasin B and phloretin (β-(4-hydroxyphenyl)-2,4,6-trihydroxypropiophenone) were purchased from *Wako*

Pure Chemical Industries and are inhibitors of nonselective facilitative glucose transporter (Glut) and an inhibitor of Glut1, respectively.[23] HIF-1α inhibitor, YC-1 (3-[5′-hydroxymethyl-2′-furyl]-1-benzyl indazole), obtained from Enzo Life Science (Farmingdale, NY). YC-1 is described to decrease HIF-1α accumulation and HIF-1 target gene expression, with the HIF-1 inhibitory effect of YC-1.[24] $CoCl_2$ is described to induce Glut1 up-regulation by the induction of HIF-1α.[25,26] mTOR inhibitors, Ku-0063794 and temsirolimus were purchased from Chemdea (Ridgewood, NJ) and LC Laboratories (Woburn, MA), respectively. Ku-0063794 is dual mTOR complex1 (mTORC1)/mTORC2 and temsirolimus inhibits only mTORC1. Anti-GLUT1 antibody was purchased from Abcam (Cambridge, MA) and anti-HIF-1α antibody was purchased from NOVUS Biologicals (Littleton, CO). Anti-β-actin antibody and anti-EGFR antibody were purchased from Santa Cruz Biotechnology (Santa Cruz, CA). Antibodies against phospho-EGFR, ERK1/2, phospho-ERK1/2, Akt, phospho-Akt, S6 Ribosomal protein, phospho-S6 Ribosomal protein, mTOR, phospho-mTOR were purchased from Cell Signaling Technology (Beverly, MA). Antibodies against HIF-1α, GLUT1 and hexokinase I were described in Section 2.3.

2.7. In vitro growth-inhibition assay

The chemosensitivity of each cell line to cisplatin was estimated by using the 3-(4,5-dimethylthiazol-2yl)-2,5-diphenyltetrazoliumbromide (MTT) assay as described previously.[27] Briefly, a 180 μL volume of an exponentially growing cell suspension was seeded into each well of a 96-well microculture plate containing 10% FBS medium and incubated for 24 h. The cells were exposed to 20 μL of each inhibitor at various concentrations and further cultured at 37 °C in a humidified atmosphere for 72 h. After the culture period, 20 μL MTT solution (5 mg/mL in phosphate-buffered saline) was added to each well and the plates were incubated for further 4 h at 37 °C. After centrifuging the plates at 200 g for 5 min, the medium was aspirated from each well, and 200 μL of DMSO was added to each well to dissolve the formazan. The growth-inhibitory effect of each inhibitor was assessed spectrophotometrically (Model 680 microplate plate reader; Bio-Rad Laboratories, Hercules, CA). Each experiment was carried out in six replicate wells for each drug concentration and carried out independently three times.

2.8. Immunoblot analysis

The cultured cells were washed twice with ice-cold PBS and lysed in M-PER mammalian protein extraction reagent (Pierce Chemical Co., Rockford, IL) with ethylene diamine tetra-acetic acid (EDTA) free Halt protease inhibitor cocktail and Halt phosphatase inhibitor cocktail (Pierce Chemical Co., Rockford, IL). Nuclear proteins were extracted with NE-PER Nuclear and Cytoplasmic Extraction Reagents (Pierce Chemical Co.) according to the manufacturer's instructions. Equal amount of protein (20 μg) in whole cell lysate [as measured by utilising the BCA protein assay reagent (Pierce Chemical Co.)] was separated by 10% SDS–PAGE and transferred to nitrocellulose membranes. Membranes were blocked with 5% skimmed milk in Tris-buffered saline-Tween 20 (TBST) for 1 h at room temperature (RT) and then incubated overnight with primary antibodies in TBST containing 5% skimmed milk at 4°C. After washing the membranes with TBST three times, they were incubated with secondary antibodies conjugated to horseradish peroxidase for 1 h at RT, followed by three washes in TBST. Immunoreactive bands were visualised by enhanced chemiluminescence (*Pierce Chemical* Co.).

2.9. ^{18}F-FDG uptake study

The cells (approximately $10–20 \times 10^4$ cells) were seeded in 24-well plates. The ^{18}F-FDG uptake studies were performed using the following medium: glucose-free RPMI-1640 with glutamine, penicillin and streptomycin. ^{18}F-FDG of 200 kBq was added to the cells and incubated for 15, 60 and 180 min at 37 °C, followed by the removal of the medium, and then the cells were washed with PBS, and lysed in 300 μL of 0.2 M NaOH. To measure the cell-bound radioactivity, an aliquot of 150 μL lysates were measured with a well-type gamma counter (ARC-7001; Aloka Co., Ltd., Tokyo, Japan), and the rest was used for protein quantification analysis (Modified Lowry Protein Assay Reagent; Pierce Chemical Co.). ^{18}F-FDG uptake was defined as follows; Uptake/mg protein (%) = cell-bound radioactivity per wells/added radioactivity/protein (mg) per wells.

2.10. Effect of Glut1, HIF-1α inhibitor, HIF-1α inducer and mTOR inhibitors on ^{18}F-FDG uptake

Cultured cells were incubated for 18 h either in the presence of $CoCl_2$ (200 μM) or YC-1 (50 μM). The cells were washed with PBS, and glucose-free RPMI-1640 was added. Cells were incubated in the presence of phloretin (200 μM) and cytochalasin B (10 μM). To examine the effect of mTOR inhibitors on ^{18}F-FDG uptake, moreover, cell cultures were also incubated for 6 h or 24 h in the presence of mTOR inhibitors (0.1, 1, 10 μM). The cells were washed with PBS, and glucose-free RPMI-1640 containing mTOR inhibitors (0.1, 1, 10 μM) was added. Then, ^{18}F-FDG of 200 kBq was added to these cells and incubated for 60 min at 37 °C. After this incubation period, the medium was then removed, and the cells were washed with PBS. Cells were

lysed in 300 μL of 0.2 M NaOH. ^{18}F-FDG uptake was measured by the procedure described above.

2.11. Statistical analysis

Probability values of <0.05 indicated a statistically significant difference. Fisher's exact test was used to examine the association of two categorical variables. Correlation of different variables was analysed using the nonparametric Spearman's rank test. The Kaplan–Meier method was used to estimate survival as a function of time, and survival difference wasanalysed by the log-rank test. Statistical analysis was performed using JMP 8 (SAS, Institute Inc., Cary, NC, USA) for Windows.

3. Results

3.1. ^{18}F-FDG PET findings and survival analysis

The median value of T/M ratio was 4.23 (range, 0.95–9.43). A median value of 4.23 was used as the cut-off T/M ratio in the following analyses, and the T/M ratio in more than 4.23 was defined as high expression. The incidence of patients with a high T/M ratio was significantly higher in stage III–IV than stage I–II ($p = 0.0075$). The mean of T/M ratio demonstrated no significant difference between patients with a histology of epithelial type (3.93 ± 0.52) and those with non-epithelial type (4.94 ± 1.33) ($p = 0.4008$).

Median survival time (MST) for all patients was 21.0 months, and the 2-year survival rate was 39.2%. The MST of patients with a low T/M ratio (⩽4.23) and those with a high T/M ratio (>4.23) on ^{18}F-FDG PET were 31.2 and 15.3 months, respectively ($p = 0.0048$) (Fig. 1).

Next, we performed the comparative analysis using maximal SUV (SUV_{max}) instead of T/M ratio. The median value of SUV_{max} was 5.20 (range, 1.45–13.2). The value of SUV_{max} was significantly correlated with that of T/M ratio ($\gamma = 0.968$, $p < 0.001$). When a median value of 5.20 was defined as cutoff SUV_{max}, the SUV_{max} of patients with stage III–IV was significantly higher than that with stage I–II ($p = 0.004$) and the MST of patients with a high SUV_{max} was significantly shorter than that with a low SUV_{max} (17.4 versus 27.2 months, $p = 0.027$). No statistically significant difference in the SUV_{max} was observed between patients with epithelial and non-epithelial type.

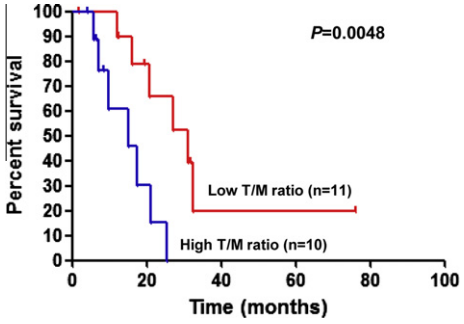

Fig. 1. Overall survival curve according to the ratio of the peak standardised uptake value of the tumour to the mean standardised uptake value of the mediastinum (T/M ratio). Overall survival of patients with high T/M ratio was significantly longer than those with low T/M ratio.

3.2. Immunohistochemical analysis

Glut1 and Glut3 were detected in tumour cells and localised predominantly on their plasma membrane. A positive rate of Glut1 and Glut3 expression was recognised in 66.7% and 90.5%, respectively. A positive expression of HIF-1α was predominantly expressed in the cytoplasm with some nuclear staining, and was recognised in 90.5%. A positive expression of hexokinase I was expressed in the cytoplasm and/or membrane of neoplastic, and was recognised in 76.2%. The median value of Ki-67 labelling index was 28% (range, 5–65%). The median rate of VEGF positivity was 70.0% (range, 25–88%), and the median numbers of CD34 was 29 (12–58). A positive expression of EGFR, PTEN, p-AKT, p-mTOR, p-S6K and Rb was 52.4%, 47.6%, 61.9%, 47.6%, 85.7% and 47.6%, respectively. High expression of p53 and bcl-2 was recognised in 66.7% and 47.6%, respectively.

3.3. Relationship between ^{18}F-FDG uptake and different variables

The results of the statistical correlation between T/M ratio and different variables are listed in Table 1. Glut1, hexokinase I, VEGF, CD34, p53 and staging yielded a statistically significant positive correlation. Using Spearman rank correlation, the T/M ratio was significantly correlated with Glut1, HIF-1α, hexokinase I, VEGF, CD34, Ki-67, p-mTOR and p53 (Table 2). In the analysis using SUV_{max}, whereas, these biomarkers were also closely correlated with the value of SUV_{max}.

3.4. ^{18}F-FDG uptake in malignant mesothelioma cell lines

Cellular ^{18}F-FDG uptake was observed in malignant mesothelioma cell line (MSTO-211H, NCI-H28 and NCI-H2052) (Fig. 2A). Effect of Glut1 inhibitor (cytochalasin B and phloretin), HIF-1α inhibitor (YC-1) and HIF-1α inducer ($CoCl_2$) on the ^{18}F-FDG uptake into malignant mesothelioma cells was evaluated (Fig. 2B and C). ^{18}F-FDG uptake in the groups treated with Glut1 inhibitors or HIF-1α inhibitor was significantly lower than the control (no treatment). On the other hand, $CoCl_2$ treatment induced an increase in ^{18}F-FDG uptake in all groups. Immunoblot analysis

Table 1
Relationship between T/M ratio of ^{18}F-FDG uptake and different variables.

Variables		T/M ratio of ^{18}F-FDG uptake		
		Low ($n = 11$)	High ($n = 10$)	p-value
Age	⩽65 year/>65 year	4/7	5/5	0.6699
Gender	Male/female	10/1	8/2	0.5864
Staging	I + II/III + IV	8/3	1/9	0.0075
Glut1	Positive/negative	4/7	9/1	0.0237
Glut3	Positive/negative	10/1	9/1	1.000
HIF-1α	Positive/negative	9/2	10/0	0.4761
Hexokinase I	Positive/negative	6/5	10/0	0.0350
VEGF	High/low	2/9	8/2	0.0089
CD34	High/low	2/9	9/1	0.0019
Ki-67	High/low	4/7	7/3	0.1983
EGFR	High/low	5/6	6/4	0.6699
PTEN	High/low	5/6	5/5	1.000
p-Akt	High/low	6/5	7/3	0.6594
p-mTOR	High/low	4/7	6/4	0.3948
pS6K	High/low	8/3	10/2	0.2142
p53	High/low	4/7	9/7	0.0237
bcl-2	High/low	6/5	4/6	0.6699
Rb	High/low	3/8	7/3	0.0860

Abbreviation: Glut1, glucose transporter 1; Glut3, glucose transporter 3; HIF-1α, hypoxia inducible factor-1 alpha; VEGF, vascular endothelial growth factor; EGFR, epidermal growth factor receptor; PTEN, phosphatase and tensin analogue; Rb, retinoblastoma protein.

Table 2
Correlation between T/M ratio of ^{18}F-FDG uptake and immunohistochemical markers.

Variables	Spearman γ	95% confidence interval	p-value
Glut1	0.7765	0.5085–0.9073	<0.0001
Glut3	0.3618	0.0964–0.6935	0.1070
HIF-1α	0.5789	0.1830–0.8133	0.0060
Hexokinase I	0.7176	0.4028–0.8806	0.0002
VEGF	0.6554	0.2994–0.8512	0.0013
CD34	0.7380	0.4385–0.8900	0.0001
Ki-67	0.5920	0.2022–0.8199	0.0047
EGFR	0.3247	–0.1380–0.6710	0.1510
PTEN	–0.0620	–0.4914–0.3916	0.7984
p-Akt	0.3042	–0.1602–0.6583	0.1801
p-mTOR	0.4366	–0.0076–0.7370	0.0478
pS6K	0.2449	–0.2220–0.6205	0.2846
p53	0.7032	0.3781–0.8739	0.0004
bcl-2	–0.4073	–0.7202–0.0433	0.0669
Rb	0.2767	–0.1893–0.6410	0.2247

Abbreviation: Glut1, glucose transporter 1; Glut3, glucose transporter 3; HIF-1α, hypoxia inducible factor-1 alpha; VEGF, vascular endothelial growth factor; EGFR, epidermal growth factor receptor; PTEN, phosphatase and tensin analogue; Rb, retinoblastoma protein.

revealed that $CoCl_2$ treatment induced an increase in HIF-1α and Glut1 protein in all cell lines though a modest increase was observed in NCI-H28 cells which harbour *VHL* gene mutation resulting in constitutive HIF-1α activation (Fig. 2D).

3.5. Evaluation of mTOR inhibitors in malignant mesothelioma cell lines

Next, based on a significant correlation between ^{18}F-FDG uptake and the expression of mTOR in our immunohistochemical analysis, we investigated whether mTOR is associated with the mechanism of ^{18}F-FDG uptake within the mesothelioma cells. This led us to the idea that mTOR inhibition in malignant mesothelioma would be a novel therapeutic option. The malignant mesothelioma cells were treated with mTOR inhibitors (Ku-0063794 and temsirolimus) (Figs. 3A and S2A) and HIF-1α inhibitor (YC-1) (Fig. 3B). Ku-0063794 treatment demonstrated potential growth inhibition in all three cell lines (Fig. 3A) whereas temsirolimus treatment demonstrated an inhibition of cell growth in MSTO-211H (Fig. S2A). The significant growth inhibition by YC-1 in NCI-H28 cells is consistent with the fact that they harbour the *VHL* gene mutation, which constitutively activates HIF-1α (Fig. 3B).

3.6. Effect of mTOR inhibitors on downstream molecules and ^{18}F-FDG uptake

Effect of Ku-0063794 on the downstream molecules was evaluated by immunoblot assay (Fig. 4A). We observed complete shutdown of phopho-S6 which is a well-known readout on mTOR inhibition and in addition, we observed the shutdown of phospho-Akt as well. In contrast, temsirolimus treatment resulted in only phopho-S6 shutdown and no effect was observed on phospho-Akt (Fig. S2B). We moved on to investigate whether ^{18}F-FDG uptake reflects these phenomena by Ku-0063794 treatment in malignant mesothelioma cells. Ku-0063794 treatment resulted in significant decrease in ^{18}F-FDG uptake in MSTO-211 and NCI-H2052 cells and this is consistent with the results of growth-inhibitory assay and immunoblot analysis. On the other hand,

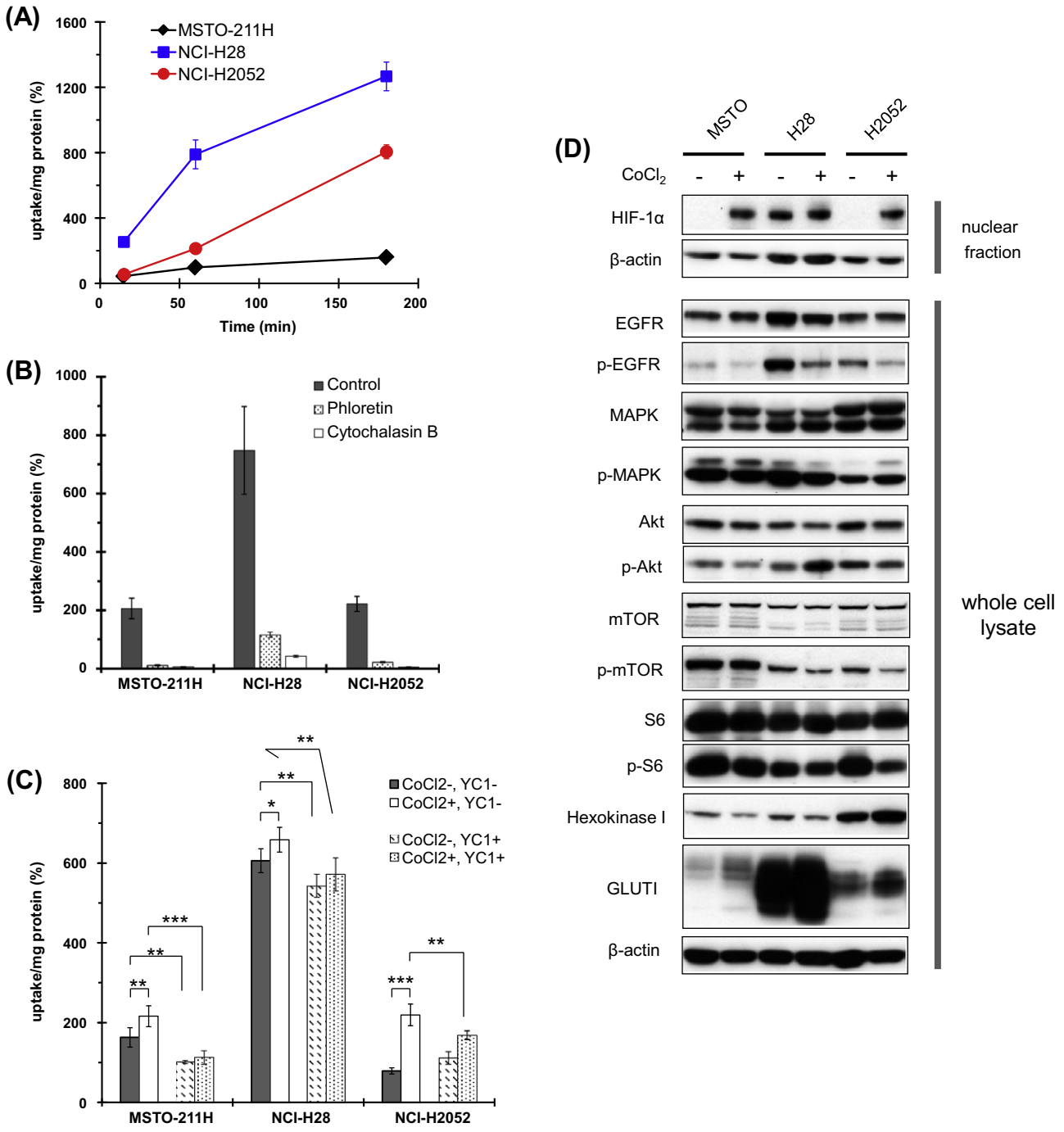

Fig. 2. ^{18}F-FDG uptake in human malignant mesothelioma cell lines. (A) Comparison of ^{18}F-FDG uptake among human malignant mesothelioma cell lines MSTO-211H, NCI-H28 and NCI-H2052. (B) Effect of Glut1 inhibitors (phloretin and cytochalasin B) on the ^{18}F-FDG uptake into human malignant mesothelioma cell lines. Phloretin and cytochalasin B, each treatment significantly attenuated ^{18}F-FDG uptake in all three human malignant mesothelioma cell lines. Data are shown as mean ± SD. (C) Effect of hypoxia inducible factor-1 alpha (HIF-1α) inducer (Cobaltous chloride) on the ^{18}F-FDG uptake into human malignant mesothelioma cell lines. $CoCl_2$ treatment induced an increase in ^{18}F-FDG uptake and its effect was counteracted by HIF-1α inhibitor YC-1. *P* values indicate significance and were calculated using Student's *t* test. *, $P < 0.05$; **, $P < 0.01$; ***, $P < 0.001$. (D) HIF-1α inducer $CoCl_2$ increases HIF-1α and GLUT1 expression levels resulting in an increase in ^{18}F-FDG uptake. MSTO-211H, NCI-H28 and NCI-H2052 cells were treated with or without $CoCl_2$ (200 μmol/L) for 18 h. Twenty micrograms each of cell lysate was subjected to immunoblot analysis with antibodies against HIF-1α, epidermal growth factor receptor (EGFR), p-EGFR, MAPK, p-MAPK, Akt, p-Akt, mTOR, p-mTOR, S6, p-S6, hexokinase I, glucose transporter 1 (GLUT1) and β-actin. $CoCl_2$ treatment induced a significant increase in HIF-1α and GLUT1 levels in MSTO-211H and NCI-H2052 cells whereas it induced a modest increase in those in NCI-H28 cells which harbour *VHL* gene mutation.

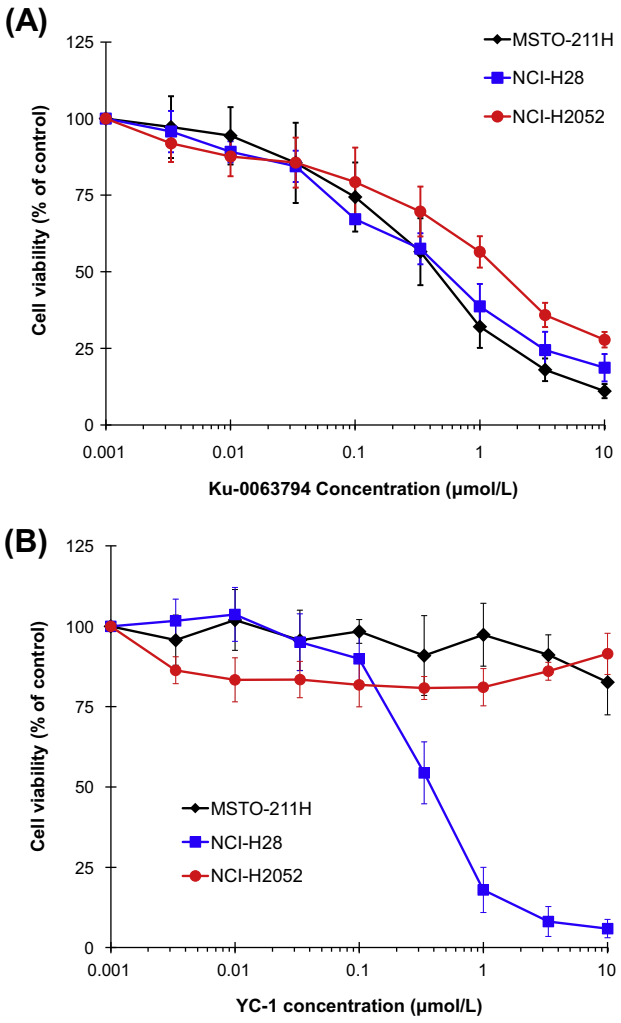

Fig. 3. Growth-inhibitory effect of mTOR inhibitor Ku-0063794 (A) and hypoxia inducible factor-1 alpha (HIF-1α) inhibitor YC-1 (B) in human malignant mesothelioma cell lines by MTT assay. Results are representative of at least three individual experiments. Data are shown as mean ± SD.

no change in ^{18}F-FDG uptake was detected in *VHL* mutant NCI-H28 cells (Fig. 4B).

4. Discussion

This is the first study to evaluate the biological correlation of ^{18}F-FDG uptake on PET in MPM. There was a statistically significant relationship between ^{18}F-FDG activity and the expression of Glut1, HIF-1α, hexokinase I, VEGF, CD34, Ki-67, mTOR and p53. ^{18}F-FDG uptake is useful for predicting disease staging and poor outcome in MPM. *In vitro* study with malignant mesothelioma cell lines demonstrated that the uptake of ^{18}F-FDG was markedly decreased by the inhibition of Glut1 or HIF-1α, whereas Glut1 upregulation by the induction of HIF-1α increased the ^{18}F-FDG uptake. Although

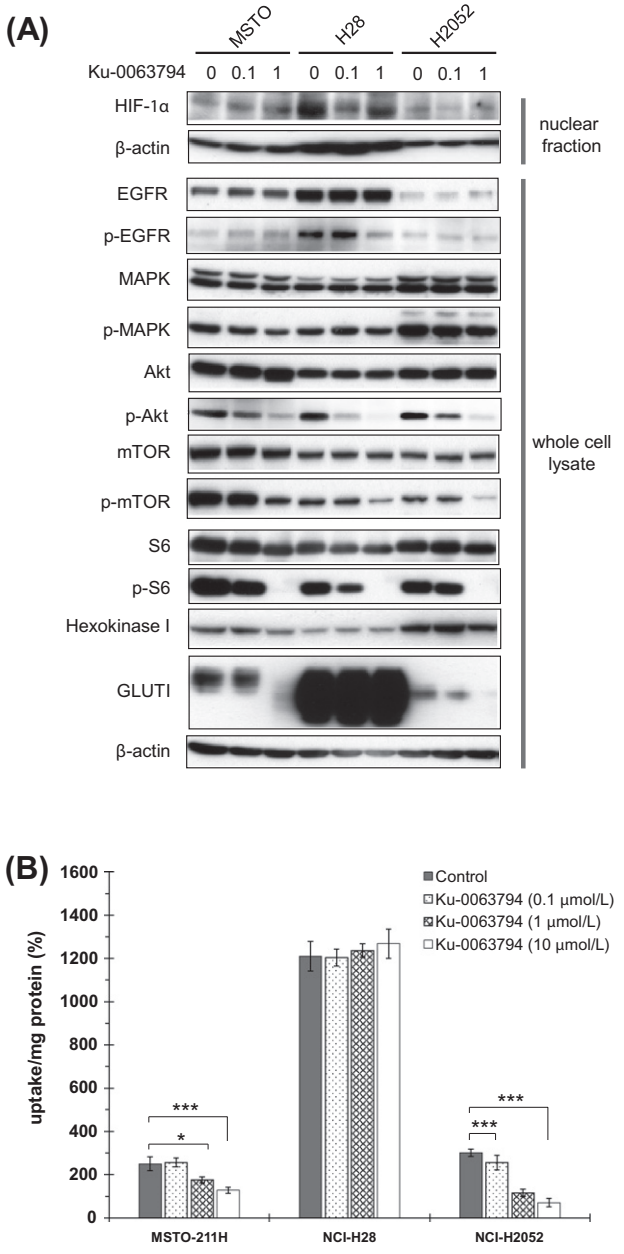

Fig. 4. Effect of mTOR inhibitor Ku-0063794 in human malignant mesothelioma cell lines. (A) MSTO-211H, NCI-H28 and NCI-H2052 cells were treated with Ku-0063794 for 6 h at indicated concentrations (0, 0.1, 1 μmol/L) and 20 μg each of cell lysate was subjected to immunoblot analysis with antibodies against hypoxia inducible factor-1 alpha (HIF-1α), epidermal growth factor receptor (EGFR), p-EGFR, MAPK, p-MAPK, Akt, p-Akt, mTOR, p-mTOR, S6, p-S6, hexokinase I, glucose transporter 1 (GLUT1) and β-actin. Ku-0063794 blocked the phosphorylation of Akt and S6 in all three cell lines and abolished GLUT1 expression in MSTO-211H and NCI-H2052. (B) Effect of Ku-0063794 on the ^{18}F-FDG uptake into human malignant mesothelioma cell lines. Each cell line was pretreated with indicated concentration of Ku-0063794 for 24 h. Significant decrease in ^{18}F-FDG uptake upon Ku-0063794 pretreatment was observed in MSTO-211H and NCI-H2052 cells in a dose-dependent manner whereas no effect was observed in NCI-H28 cell line. *P* values indicate significance and were calculated using Student's *t* test. $^{*}P < 0.05$; $^{**}P < 0.01$; $^{***}P < 0.001$.

Glut1 or HIF-1α is a downstream component of mTOR signalling pathway, our *in vitro* study demonstrated that mTOR pathway is related to the mechanism of ^{18}F-FDG uptake within malignant mesothelioma cell.

Imaging of MPM plays a critical role on the diagnosis, outcome, prediction or assessment of response to chemotherapy, and monitoring of disease recurrence after surgery.[28] At these points, ^{18}F-FDG PET is useful modality and has a high sensitivity and specificity for differentiation of benign from malignant pleural disease. Recent studies have addressed the clinical significance of ^{18}F-FDG PET imaging in patients with MPM. On the other hand, improvement in our understanding of the molecular biology of MPM has identified promising new therapies and pathways that are candidates for targeted therapies. Recent reviews have been described that the molecular biomarkers including VEGF, EGFR, p53, pRb and bcl-2 appear to play an important role in the pathogenesis and prognosis of MPM.[17,29] Glut1 and HIF-1α have been documented to be a useful immunohistochemical marker in the differential diagnosis of benign reactive mesothelium from MPM.[30,31] Our study indicates that the mechanism behind ^{18}F-FDG accumulation in MPM depends upon the overexpression of glucose transporter and the relative amounts of hexokinase, and their upregulation in hypoxic condition. Moreover, our study suggests that the overexpression of HIF-1 promotes angiogenesis and metabolic adaptation of malignant mesothelioma cells, and the HIF-1 oxygen-sensing system results in the development of tumour growth, invasion and metastasis.

Recent studies have documented that ^{18}F-FDG uptake is closely linked with the antitumour activity of the mTOR inhibitor and is a useful pharmacodynamic marker in cancer patients treated by mTOR inhibitors.[12,16,32] However, the other report has described that ^{18}F-FDG–PET is not a useful predictive marker to mTOR inhibitor therapy but a pharmacodynamic marker for Akt activation during mTOR inhibitor therapy.[33] Some researchers have documented that mTOR mediates survival signals in many mesothelioma and targeting mTOR signalling pathways may have significant therapeutic value in MPM patients.[34,35] The present study indicated that mTOR inhibitor could decrease the expression of Glut1 via the uptake of ^{18}F-FDG within the MPM cells and mTOR signalling pathway has a significant relationship with ^{18}F-FDG uptake. Of three mesothelioma cell lines, two (MSTO-H211 and NCI-H2052) had a decreased uptake of ^{18}F-FDG by mTOR inhibitors, but one with the *VHL* mutation (NCI-H28) had no decreased ^{18}F-FDG accumulation. mTOR complexes with the raptor and rictor proteins to form mTOR complex 1 (mTORC1) and mTORC2, respectively.[36] mTORC1 regulates growth and cell cycle progression via downstream mediators such as p70S6K. mTORC2 is an upstream component of PI3K/Akt pathway and regulates Akt activity. Ku-0063794 is a dual mTORC1/mTORC2 inhibitor unlike temsirolimus which inhibits only mTORC1 signalling, suggesting that inhibition of mTORC1 may not be enough and dual mTORC1/mTORC2 inhibition may be necessary for growth inhibition in malignant mesothelioma cells. Moreover, mTORC1 and mTORC2 seem to be strongly related to the mechanism of Glut1 expression and ^{18}F-FDG uptake within mesothelioma cell as compared with mTORC1 alone. Therefore, these results suggest that ^{18}F-FDG–PET may be utilised as a tool for predicting the response to mTOR inhibitors, especially dual mTORC1/mTORC2 inhibitors in malignant mesothelioma patients except those harbouring the *VHL* gene mutation. Although temsirolimus is active against mesothelioma *in vitro* and *in vivo*,[37] there is still no data about the efficacy of dual mTORC1/mTORC2 inhibitor against mesothelioma cell. Moreover, it remains unknown whether the mechanism of ^{18}F-FDG uptake is associated with mTOR signalling pathway. To clearly identify the mechanism of ^{18}F-FDG uptake in tumour cell, the results of our study may be meaningful in patients with human neoplasms including MPM.

The Warburg effect is the best characterised metabolic phenotype observed in tumour cells. It is defined as an increased dependence on glycolysis for ATP synthesis and decreased mitochondrial oxidative phosphorylation. This effect is regulated by the PI3K/AKT, HIF, p53, MYC and AMP-activated protein kinase (AMPK)-liver kinase B1 (LKB1) pathways.[38] HIF-dependent metabolic changes are a major determinant of the glycolytic downstream of PI3K, AKT1 and mTOR. Our results suggest that the PI3K/AKT/mTOR signalling pathway plays a crucial role in the glycolytic system related to ^{18}F-FDG uptake. Thus, further study is necessary for examining whether ^{18}F-FDG uptake by the activity of these molecules is associated with the Warburg effect.

The present study has several limitations. Firstly, our population was of a small sample size, therefore the present study warrants a larger, multicentre cohort study. Another limitation is that all of 21 patients with MPM in our study have not been treated with mTOR inhibitor, therefore we have no clinical data about the relationship between ^{18}FDG uptake and the inhibition of mTOR in MPM. However, there is still no data about the efficacy of mTOR inhibitor in patients with MPM.

In conclusion, glucose metabolism, hypoxia, angiogenesis, cell proliferation, cell cycle control and mTOR signalling pathway play an important role for the mechanism of ^{18}F-FDG uptake within malignant mesothelioma cell. HIF-1α is upregulated by hypoxia and induces Glut1 expression and angiogenesis. Microvessels provide ^{18}FDG uptake, Glut1 transports ^{18}FDG into the tumour cell, and hexokinase enters ^{18}FDG into glycolysis. As a result of tumour cell proliferation and upregulation of cell cycle, the amount of ^{18}FDG within the

tumour cells is increasing. Our *in vitro* data suggest that mTOR activation is associated with the upregulation of Glut1 expression and ^{18}FDG uptake, and mTOR inhibition is a promising novel therapeutic agent against MPM. We believe that the biological correlation of ^{18}FDG accumulation within tumour cells leads to a more rationale use of PET scanning in patients with MPM.

Conflict of interest statement

None declared.

Acknowledgements

This work was supported in part by Grant 21790793 (K.K) from the Ministry of Education, Culture, Sports, Science and Technology, Japan, and National Hospital Organisation Policy Based Medical Services. We thank Mrs. Akane Naruoka for her technical assistance of *in vitro* analysis and all staffs of pathology department in Shizuoka Cancer Center for their technical assistance of immunohistochemical analysis.

Appendix A. Supplementary data

Supplementary data associated with this article can be found, in the online version, at doi:10.1016/j.ejca.2012.01.016.

References

1. Benard F, Sterman D, Smith RJ, et al. Metabolic imaging of malignant pleural mesothelioma with fluorodexyglucose positron emission tomography. *Chest* 1998;**114**:713–22.
2. Benard F, Sterman D, Smith RJ, et al. Prognostic value of FDG PET imaging in malignant pleural mesothelioma. *J Nucl Med* 1999;**40**:1241–5.
3. Yildirim H, Metintas M, Entok E, et al. Clinical value of fluorodeoxyglucose-positron emission tomography/computed tomography in differentiation of malignant mesothelioma from asbestos-related benign pleural disease: an observational pilot study. *J Thorac Oncol* 2009;**4**:1480–4.
4. Ceresoli GL, Chiti A, Zucali PA, et al. Early response evaluation in malignant pleural mesothelioma by positron emission tomography with [^{18}F]fluorodeoxyglucose. *J Clin Oncol* 2008;**24**:4587–93.
5. Carretta A, Landoni C, Melloni G, et al. 18-F FDG positron emission tomography in the evaluation of malignant pleural diseases: a pilot study. *Eur J Cardiothorac Surg* 2000;**17**:377–83.
6. Flores RM, Akhurst T, Gonen M, et al. Positron emission tomography predicts survival in malignant pleural mesothelioma. *J Thorac Cardiovasc Surg* 2006;**132**:763–8.
7. Higashi K, Ueda Y, Sakurai A, et al. Correlation of Glut-1 glucose transporter expression with [^{18}F] FDG uptake in non-small cell lung cancer. *Eur J Nucl Med* 2000;**27**:1778–85.
8. Chung JH, Cho KJ, Lee SS, et al. Over expression of Glut 1 in lymphoid follicles correlates with false-positive ^{18}F-FDG PET results in lung cancer staging. *J Nucl Med* 2004;**45**:999–1003.
9. Vleugel MM, Greijer AE, Shvarts A, et al. Differential prognostic impact of hypoxia induced and diffuse HIF-1 alpha expression in invasive breast cancer. *J Clin Pathol* 2005;**58**:172–7.
10. Elson DA, Ryan HE, Snow JW, et al. Coordinate up-regulation of hypoxia inducible factor (HIF)-1a and HIF-1 target genes during multi-stage epidermal carcinogenesis and wound healing 1. *Cancer Res* 2000;**60**:6189–95.
11. Burgman P, Odonoghue JA, Humm JL, et al. Hypoxia-induced increase in FDG uptake in MCF7 cells. *J Nucl Med* 2001;**42**:170–5.
12. Thomas GV, Tran C, Mellinghoff IK, et al. Hypoxia-inducible factor determines sensitivity to inhibitors of mTOR in kidney cancer. *Nat Med* 2006;**12**:122–7.
13. Guo J, Higashi K, Ueda Y, et al. Microvessel density: correlation with ^{18}F-FDG uptake and prognosis impact in lung adenocarcinomas. *J Nucl Med* 2006;**47**:419–25.
14. Kaira K, Oriuchi N, Shimizu K, et al. Correlation of angiogenesis with ^{18}F-FMT and ^{18}F-FDG uptake in non-small cell lung cancer. *Cancer Sci* 2009;**100**:753–8.
15. Ryan HE, Polni M, McNulty W, et al. Hypoxia-inducible factor-1α is a positive factor in solid tumor growth. *Cancer Res* 2000;**60**:4010–5.
16. Novoga L, Bocellaard R, Kobe C, et al. Downregulation of ^{18}FDG uptake in PET as an early pharmacodynamic effect in treatment of non-small cell lung cancer with the mTOR inhibitor everlimus. *J Nucl Med* 2009;**50**:1815–9.
17. Lee AY, Raz DJ, He B, et al. Update on the molecular biology of malignant mesothelioma. *Cancer* 2007;**109**:1454–61.
18. Rusch VWThe International Mesothelioma Interest Group. A proposed new international TNM staging system for malignant pleural mesothelioma. *Chest* 1995;**108**:1122–8.
19. Kaira K, Endo M, Abe M, et al. Biologic correlation of 2-[^{18}F]-fluoro-2-deoxy-D-glucose uptake on positron emission tomography in thymic epithelial tumors. *J Clin Oncol* 2010;**28**:3746–53.
20. van Baardwijk A, Dooms C, van Suylen RJ, et al. The maximum uptake of ^{18}F-deoxyglucose on positron emission tomography scan correlates with survival, hypoxia inducible factor-1α and GLUT-1 in non-small cell lung cancer. *Eur J Cancer* 2007;**43**:1392–1398.
21. Chung JH, Cho KJ, Lee SS, et al. Over expression of Glut1 in lymphoid follicles correlates with false-positive ^{18}F-FDG PET results in lung cancer staging. *J Nucl Med* 2004;**45**:999–1003.
22. Riedl CC, Akhurst T, Larson S, et al. ^{18}F-FDG PET scanning correlates with tissue markers of poor prognosis and predicts mortality for patients after liver resection for colorectal metastases. *J Nucl Med* 2007;**48**:771–5.
23. Gibbs ME, Hutchinson DS, Summers RJ. Role of β-adrenoceptors in memory consolidation: β_3-adrenoceptors act on glucose uptake and β_2-adrenoceptors on glycogenolysis. *Neuropsychopharmacology* 2008;**33**:2384–97.
24. Moon SY, Chang HW, Roh JL, et al. Using YC-1 to overcome the radioresistance of hypoxic cancer cells. *Oral Oncol* 2009;**45**:915–9.
25. Hayashi M, Sakata M, Takeda T, et al. Induction of glucose transporter 1 expression through hypoxia-inducible factor 1α under hypoxic conditions in trophoblast-derived cells. *J Endocrinol* 2004;**183**:145–54.
26. Vissers MC, Gunningham SP, Morrison MJ, et al. Modulation of hypoxia-inducible factor-1 alpha in cultured primary cells by intracellular ascorbate. *Free Radical Biol Med* 2007;**42**:765–72.
27. Mosmann T. Rapid calorimetric assay for cellular growth and survival: application of proliferation and cytotoxicity assays. *J immunol Methods* 1983;**65**:55–63.
28. Nowak AK, Armato III SG, Ceresoli CL. Imaging in pleural mesothelioma: a review of imaging research presented at the 9th international meeting of the International Mesothelioma Interest group. *Lung Cancer* 2010;**70**:1–6.
29. Kumar P, Kratzke RA. Molecular prognostic markers in malignant mesothelioma. *Lung Cancer* 2005;**4951**:S53–60.
30. Kato Y, Tsuta K, Seki K, et al. Immunohistochemical detection of GLUT1 can discriminate between reactive mesothelium and malignant mesothelioma. *Mod Pathol* 2007;**20**:215–20.

31. Klabatsa A, Sheaff MT, Steele JPC, et al. Expression and prognostic significance of hypoxia-inducible 1α (HIF-1α) in malignant pleural mesothelioma (MPM). *Lung Cancer* 2006;**51**:53–9.
32. Cejka D, Kuntner C, Preusser M, et al. FDG uptake is a surrogate marker for definding the optimal biological dose of the mTOR inhibitor everolimus in vivo. *Br J Cancer* 2009;**1000**:1739–45.
33. Ma WW, Jacene H, Song D, et al. [18F]Fluorodeoxyglucose positron emission tomography correlates with Akt pathway activity but Is not predictive of clinical outcome during mTOR inhibitor therapy. *J Clin Oncol* 2009;**27**:2697–704.
34. Wilson SM, Barbone D, Yang TM, et al. MTOR mediates survival signals in malignant mesothelioma grown as tumor fragment speroids. *Am J Respir Cell Mol Biol* 2008;**39**:576–83.
35. Varghese S, Chen Z, Bartlett DL, et al. Activation of the phosphoinositide-3-kinase and mammalian target of rapamycin signaling pathways are associated with shortened survival in patients with malignant peritoneal mesothelioma. *Cancer* 2011;**117**:361–71.
36. Sabatini DM. MTOR and cancer: insights into a complex relationship. *Nat Rev Cancer* 2006;**6**:729–34.
37. Hoda MA, Mohamed A, Ghanim B, et al. Temsirolimus inhibits malignant pleural mesothelioma growth in vitro and in vivo. *J Thorac Oncology* 2011;**6**:852–63.
38. Carins RA, Harris IS, Mak TW. Regulation of cancer cell metabolism. *Nat Rev Cancer* 2011;**11**:85–95.